A Superposition Method for Representing Wellbore Crossflow in Reservoir Simulation

A.D. Modine,* K.H. Coats,** SPE, and **M.W. Wells,†** Scientific Software-Intercomp

SPE 20746

Summary. Production from highly stratified reservoirs can result in significant crossflow between layers through wellbores. This paper describes a new, relatively simple superposition method to represent this crossflow in a numerical simulator. The method calculates vertical wellbore saturation variations throughout the wellbore and gives more accurate results than a fully mixed wellbore method. Equations are given for the new method, a fully mixed wellbore method, and the exact solution for crossflow in a well completed in a column of gridblocks. Three examples, including a field-scale depletion, are given comparing exact results with those from the superposition and fully mixed wellbore methods.

Introduction

The aim of simulating wellbore and near-wellbore behavior in a field-scale model is to attain accuracy and stability with numerical efficiency. The introduction of the strongly coupled well model[1,2] provided stability by simultaneously solving the well target rate constraints with the reservoir pressure and saturation equations. Later, Holmes[3] described a fully mixed wellbore model to treat interlayer crossflow through wellbores. This approach increased accuracy in simulating highly stratified reservoirs where significant interlayer flow may occur through the wellbore of a shut-in or flowing well. However, this fully mixed approach can give erroneous saturations for the wellbore-to-formation outflow-layer flow stream because it assumes vertically uniform saturation of each phase throughout the wellbore.

This paper presents a new superposition method that includes a layer-by-layer mass balance to calculate the variation of wellbore saturations among the layers. The well target rate is allocated among perforated layers with implicit bottomhole constraints imposed to preserve that rate. Additional interlayer flow terms then are superposed on those allocated layer rates to obtain total layer rates that reflect the sum of the well target rate and crossflow.

Equations are presented describing this superposition method, a fully mixed wellbore method, and the exact solution for instantaneous layer total and individual-phase rates of a well completed in a column of gridblocks. A stand-alone program that uses these equations was run to compare the three methods for many crossflow cases having various layer properties and well rates.

An eight-layer example presented in detail illustrates the general finding that the exact results are approximated more accurately by the superposition method than by the fully mixed wellbore method.

A procedure is described whereby the simulator can be used to calculate the exact crossflow behavior for a single-well or multiwell field-scale cross section. Two examples where this procedure is used are presented that compare superposition method results with the exact behavior of a single-well shut-in transient and a 10-year field-scale depletion case.

The superposition method described here applies to black-oil or compositional simulation models. The simulator results presented were obtained from the method programmed in a fully implicit compositional model.[4]

The superposition method accounts for the role or effect of wellbore gradient. This paper, however, does not address the separate problem of formulating a general and accurate method of calculating that gradient.

Development of Equations

Consider a producing well that penetrates n contiguous grid layers and produces a target rate of q. For any individual Layer k, the total layer rate is

$$q_k=J_k\lambda_k(P_k-p_w), \quad \ldots\ldots(1)$$

where $\lambda_k=\sum_m\left(\frac{k_r}{\mu}\right)_{m,k}^{ma}, \quad m=w,o,g. \quad \ldots\ldots(2)$

Summing q_k in Eq. 1 over all layers and using the relation $\Sigma q_k=q$ allows calculation of the following wellbore pressure:

$$p_w=(\Sigma J_k\lambda_k P_k-q)/\Sigma J_k\lambda_k. \quad \ldots\ldots(3)$$

If p_w is greater than the smallest P_k, then crossflow exists with some (inflow) layers producing into the wellbore and other (outflow or crossflow) layers accepting fluid from the wellbore.

The individual phase layer rates are given by

$$q_{mk}=J_k\hat{\lambda}_{mk}(P_k-p_w), \quad m=w,o,g, \quad \ldots\ldots(4)$$

where $\hat{\lambda}_{mk}=\lambda_{mk} \quad \ldots\ldots(5)$

for an inflow layer and

$$\hat{\lambda}_{mk}=\lambda_k S_{mk}^{wb} \quad \ldots\ldots(6)$$

for an outflow layer.

The individual phase rates given in Eq. 4 can be used in steady-state phase mass balances written for each layer of the wellbore to obtain a reservoir-volume-unit wellbore mass balance that can easily be used to calculate the layer-dependent wellbore saturations, S_{mk}^{wb}. These mass balances neglect compressibility and mass-transfer effects within the wellbore and require no assignment of wellbore cell volumes. Eqs. 1, 3, and 4 then give an exact solution to the crossflow problem in terms of instantaneous total and individual-phase layer flow rates.

A mixed wellbore approximate method is similar to the above description, except that a single set of wellbore saturations, S_m^{wb}, is used in place of the layer-dependent values in Eq. 6. A total wellbore mass balance for each phase is

$$\Sigma^+ q_{mk}+\Sigma^- q_{mk}-qS_m^{wb}=0, \quad m=w,o,g, \quad \ldots\ldots(7)$$

where Σ^+ and Σ^- denote summation over inflow and outflow layers, respectively. Expansion of the outflow sum gives

$$\Sigma^+ q_{mk}+S_m^{wb}\Sigma^- J_k\lambda_k(P_k-p_w)-qS_m^{wb}=0. \quad \ldots\ldots(8)$$

Solving for the average wellbore saturation gives

$$S_m^{wb}=\Sigma^+ q_{mk}/[q-\Sigma^- J_k\lambda_k(P_k-p_w)]. \quad \ldots\ldots(9)$$

Eqs. 1 and 4, with this layer-independent, or single-saturation, set used in place of S_{mk}^{wb} given in Eq. 6, then give the approximate mixed wellbore crossflow solution. Again, no wellbore cell volumes are required to calculate the mixed wellbore saturations given in Eq. 9.

The approximate superposition method combines two calculations. First, the target rate is allocated only among inflow layers as

$$q_k^*=J_k\lambda_k(P_k-p_w^*) \text{ if } P_k>p_w^* \quad \ldots\ldots(10)$$

*Deceased.
**Now with K.H. Coats and Co. Inc.
†Now with Intera ECL-Petroleum Technologies.

TABLE 1—EXAMPLE PROBLEM PROPERTIES, EIGHT-LAYER TEST PROBLEM

Layer	Matrix Relative Permeabilities k_{ro}	k_{rg}	k_{rw}	Matrix Pressure (psia)
1	0.100	0.020	0.010	2,000
2	0.020	0.400	0.100	6,000
3	0.200	0.300	0.020	3,000
4	0.020	0.010	0.600	1,500
5	0.500	0.100	0.100	4,000
6	0.600	0.050	0.050	2,500
7	0.300	0.010	0.500	1,500
8	0	0	1.000	5,500

PI for all layers, RB-cp/D-psi	0.10
Oil viscosity, cp	0.50
Gas viscosity, cp	0.05
Water viscosity, cp	0.25

and $q_k^*=0$ if $P_k \le p_w^*$, ... (11)

with p_w^* easily determined as

$$p_w^*=(\Sigma^+ J_k\lambda_k P_k - q)/\Sigma^+ J_k\lambda_k, \quad \ldots\ldots (12)$$

where Σ^+ again denotes summation over inflow layers only. The calculation given in Eqs. 10 through 12 satisfies target rate exactly but ignores all crossflow. The second calculation seeks a form of additional interlayer (matrix layers) flow terms between Layers k and j:

$$q_{kj}=T_{kj}(\phi_k-\phi_j), \quad \ldots\ldots (13)$$

which when added to or superposed on the rates q_k^* gives an approximation to the exact crossflow solution. Eqs. 10 through 12 are straightforward, and Eq. 13 is equally simple in simulators with linear solvers accepting off-band connection terms (e.g., for faults or well-implicit bottomhole-constraint terms).

To develop the relations necessary to include Eq. 13 in a simulator, layer rates $\hat{q}_k$, which sum to zero, are defined by

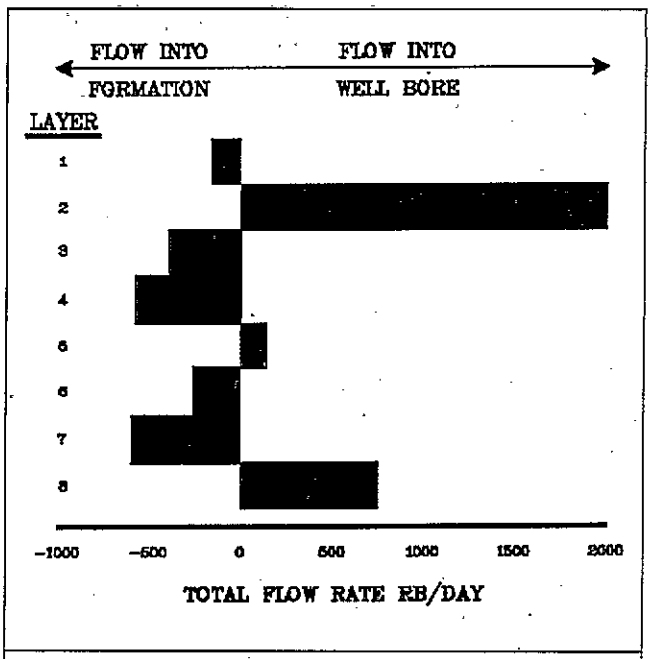

Fig. 1—Total flow rate profile for q=1,000 RB/D.

$$\hat{q}_k=J_k\lambda_k(\hat{P}_k-p_w), \quad \ldots\ldots (14)$$

where $\hat{P}_k=\min(P_k,p_w^*)$. ..... (15)

Because the $\hat{q}_k$ sum to zero,

$$p_w=\Sigma J_k\lambda_k\hat{P}_k/\Sigma J_k\lambda_k. \quad \ldots\ldots (16)$$

It can be shown that p_w from Eq. 16 exactly equals that of Eq. 3 and

$$q_k^*+\hat{q}_k=q_k \quad \ldots\ldots (17)$$

from Eq. 1.

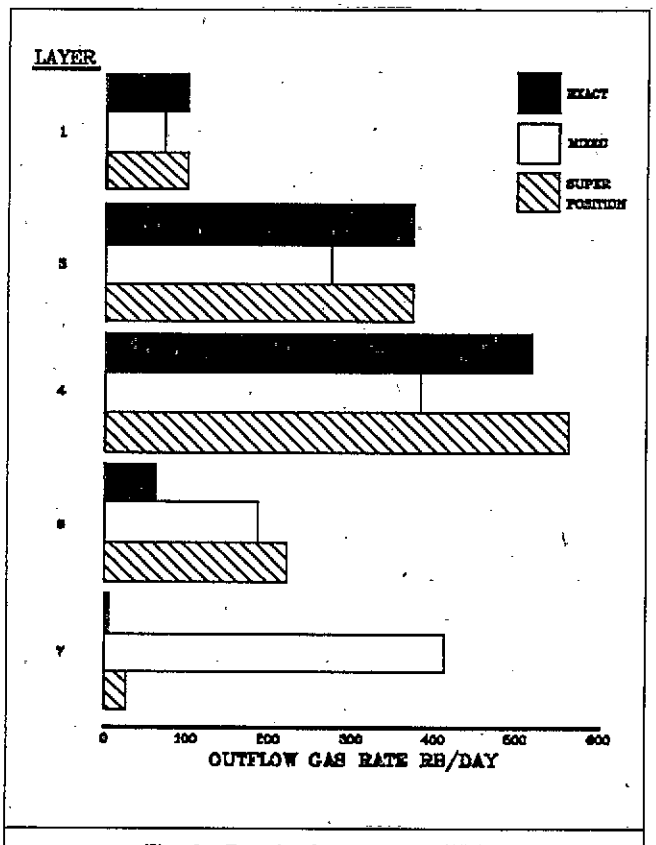

Fig. 2—Results for q=1,000 RB/D.

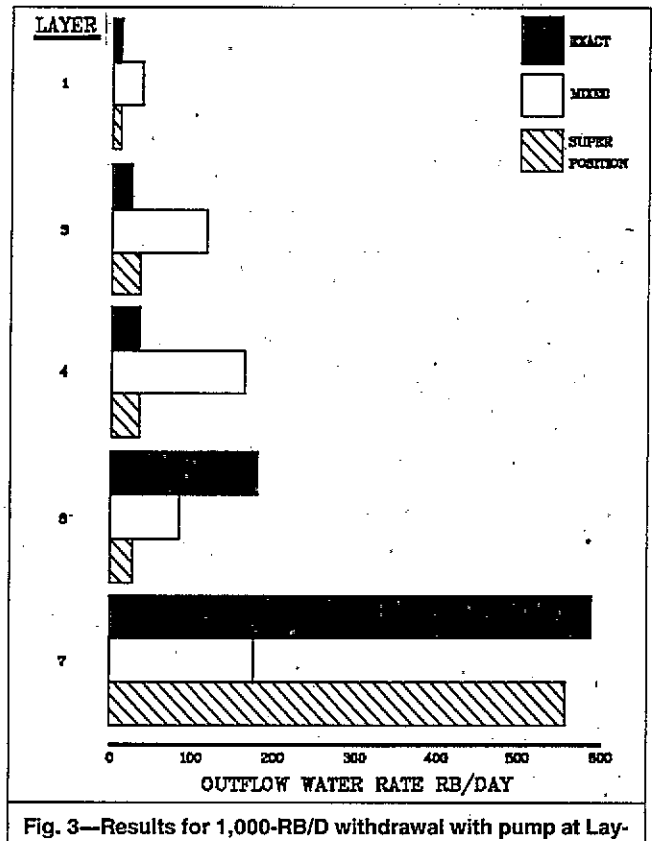

Fig. 3—Results for 1,000-RB/D withdrawal with pump at Layer 1.

TABLE 2—EXAMPLE PROBLEM CALCULATED WELLBORE SATURATIONS, EIGHT-LAYER TEST PROBLEM

	Well Production Rate at 1,000 RB/D Rate			Well Production Rate, Shut-In Well		
Layer	Oil	Gas	Water	Oil	Gas	Water
1	0.0047	0.9479	0.0474	0.0047	0.9479	0.0474
2	0.0047	0.9479	0.0474	0.0047	0.9479	0.0474
3	0.0047	0.9479	0.0474	0.0047	0.9479	0.0474
4	0.0225	0.9258	0.0517	0.0047	0.9479	0.0474
5	0.2941	0.5882	0.1176	0.0214	0.9271	0.0514
6	0.1097	0.2194	0.6709	0.0214	0.9271	0.0514
7	0	0	1.0000	0.0017	0.0736	0.9247
8	0	0	1.0000	0	0	1.0000

TABLE 3—RESERVOIR PROPERTIES FOR FIELD EXAMPLE*

Layer	Thickness (ft)	Horizontal Permeability (md)	Vertical Permeability (md)	Porosity (Fraction)
1	60	6.0	0.02	0.35
2	50	10.0	0.05	0.31
3	50	12.8	0.06	0.35
4	10	13.7	0.04	0.31
5	160	4.8	0.20	0.37
6	220	2.0	0.11	0.27

*The interblock vertical transmissibility between Layers 4 and 5 is zero, and the grid system is 16×6 with a constant x-direction grid cell size of 152 ft and a y-direction width of 2,800 ft.

Substituting p_w from Eq. 16 into Eq. 14 yields

$$\hat{q}_k = \frac{1}{\sum_j J_j \lambda_j} \sum_j J_k \lambda_k J_j \lambda_j (\hat{P}_k - \hat{P}_j). \quad \ldots\ldots\ldots\ldots\ldots (18)$$

Therefore, the superposition solution $q_k^* + \hat{q}_k$ with $\hat{q}_k$ given by Eq. 14 or 18 is identical to the exact solution for single-phase flow and for total layer rates in the multiphase case.

Comparing Eqs. 13 and 18 shows that the interblock (layer) transmissibility should be

$$T_{kj} = J_k J_j \lambda_k \lambda_j / \sum_j J_j \lambda_j \quad \ldots\ldots\ldots\ldots\ldots\ldots\ldots\ldots\ldots (19)$$

and the layer potential, ϕ_k, should be $\hat{P}_k$.

The superposition method is approximate only when applied to individual-phase outflow layer rates in the multiphase case. From Eq. 14, the individual-phase layer rates are

$$\hat{q}_{mk} = J_k \hat{\lambda}_{mk} (\hat{P}_k - p_w), \quad \ldots\ldots\ldots\ldots\ldots\ldots\ldots\ldots\ldots (20)$$

with $\hat{\lambda}_{mk}$ given by Eq. 6. The layer-dependent wellbore saturations are calculated by the mass balance with the $\hat{q}_{mk}$ rates. These wellbore saturations reflecting $\hat{q}_{mk}$ differ from the exact wellbore saturations reflecting q_{mk} from Eq. 4. The wellbore saturations, however, are identical when the well target rate is zero (crossflow is a maximum) and differ the most as the crossflow approaches zero.

Because the individual phase rates, $\hat{q}_{mk}$, sum to zero, p_w in Eq. 20 can be expressed by Eq. 16 or

$$p_w = \Sigma J_k \hat{\lambda}_{mk} \hat{P}_k / \Sigma J_k \hat{\lambda}_{mk}, \; m = w, o, g. \quad \ldots\ldots\ldots\ldots\ldots\ldots (21)$$

Substituting Eq. 21 into Eq. 20 gives the individual-phase superposition interblock (layer) rates as

$$\hat{q}_{mk} = \frac{1}{\sum_j J_j \hat{\lambda}_{mj}} \sum_j J_k \hat{\lambda}_{mk} J_j \hat{\lambda}_{mj} (\hat{P}_k - \hat{P}_j). \quad \ldots\ldots\ldots\ldots\ldots (22)$$

In the simulator, the right-side mass interlayer phase flow rates given in Eq. 22 are calculated with the addition of upstream phase densities and the use of implicit upstream $\hat{\lambda}_m$ and explicit downstream $\hat{\lambda}_m$. No effect of the latter explicit term on convergence rate has been noticed. The potential $\hat{P}_k$ terms are taken implicitly.

TABLE 4—MISCELLANEOUS PROPERTIES FOR FIELD EXAMPLE

Rock compressibility, psi^{-1}	8.8×10^{-6}
Water compressibility, psi^{-1}	3.02×10^{-6}
Water viscosity, cp	0.22
Water FVF at initial pressure of 6,568.4 psia, RB/STB	1.035
Water density at stock-tank conditions, lbm/ft^3	63.65
Reservoir temperature, °F	245
Top of formation, ft ss*	9,186.4
GOC, ft ss	9,335
WOC, ft ss	10,050
Initial pressure at 9,335 ft, psia	6,568.4

*ss = subsea.

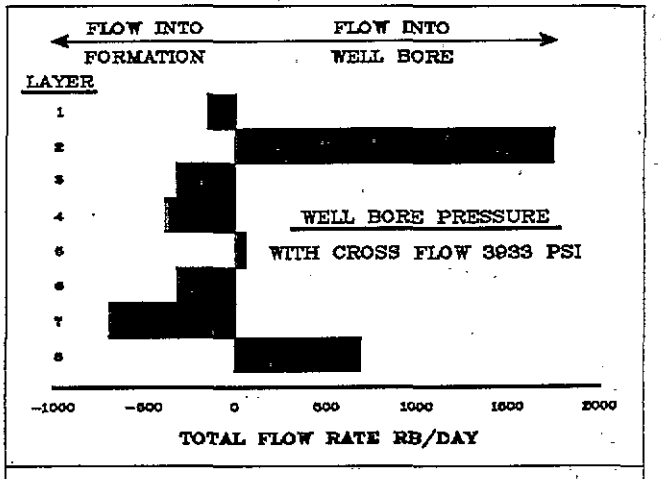

Fig. 4—Total flow rate profile for shut-in well.

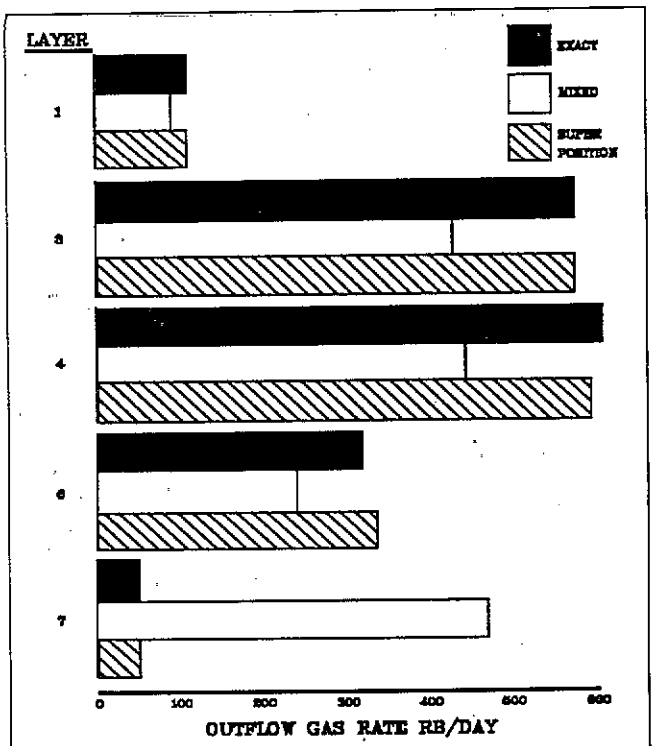

Fig. 5—Gas rate results for shut-in well.

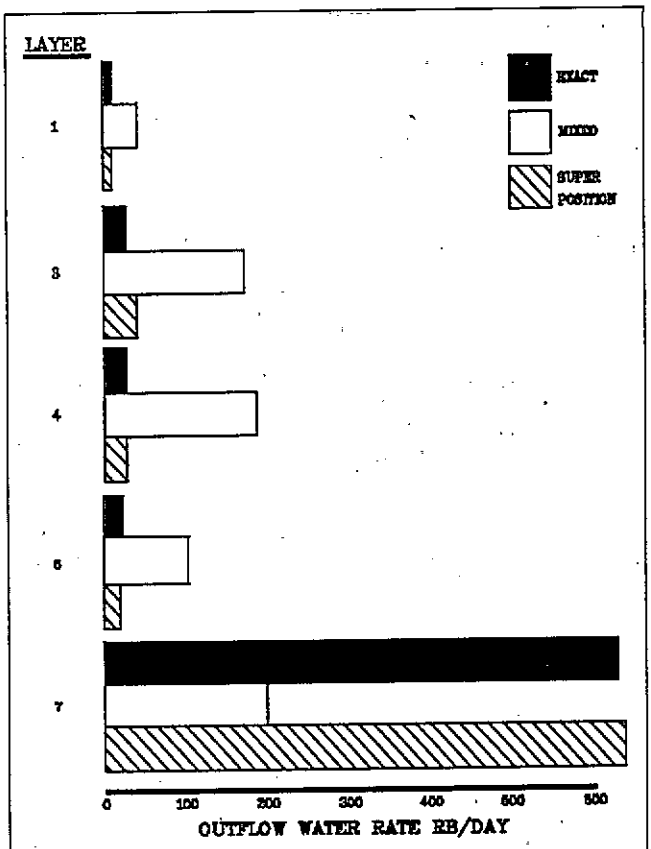

Fig. 6—Water rate results for shut-in well.

For all inflow layers, the superposition method is identical to the exact solution for both total and individual-layer phase rates. For cases with more than one outflow (crossflow) layer, the method is approximate because at least one term (each outflow pair term) in Eq. 22 contains a layer upstream value for $\hat{\lambda}_m$ when it should contain the wellbore $\hat{\lambda}_m$ value.

Inspection of the above equations shows that all three methods give the same inflow-layer total and individual-phase rates. They also give the same outflow-layer total rates. They differ only in the individual-phase layer outflow rates.

Discussion

The superposition method (Eqs. 10 through 22 above) applies for target rate q expressed in any units. For any such units, the target rate calculation for p_w^* is an iterative calculation, which is a necessary capability of any numerical simulator. After that p_w^* calculation, Eqs. 10 and 11 apply in units of reservoir barrels per day and the method continues as above.

For the injection-well case, the above equations and logic apply with trivial differences. The only basic difference is that the well rate q is negative and must be identified by phase.

The presence of wellbore-gradient effects in the above equations is a simple consequence of the definition of P_k. The wellbore pressure gradient equation is

$$p_{wk}=p_w+\Delta p_{wk}, \quad \ldots\ldots\ldots\ldots\ldots\ldots\ldots\ldots\ldots\ldots\ldots\ldots (23)$$

where p_w is wellbore pressure at some arbitrary Layer k^* and Δp_{wk} is $p_{wk}-p_w$. The layer rate is

$$q_k=J_k\lambda_k(p_k-p_{wk})=J_k\lambda_k(p_k-p_w-\Delta p_{wk}), \quad \ldots\ldots\ldots\ldots\ldots (24)$$

and with the definition $P_k\equiv p_k-\Delta p_{wk}$, Eq. 24 becomes Eq. 1.

There are many different ways of calculating or estimating the wellbore gradient, Δp_{wk}, a topic not addressed in this paper.

Testing the Superposition Method

Instantaneous Crossflow Rates. The accuracy of the superposition method was examined first by comparing instantaneous (steady-state) layer rates for the exact, mixed-wellbore, and superposition methods. A stand-alone program based on Eqs. 1 through 22 was written to calculate these rates for the three methods. This program

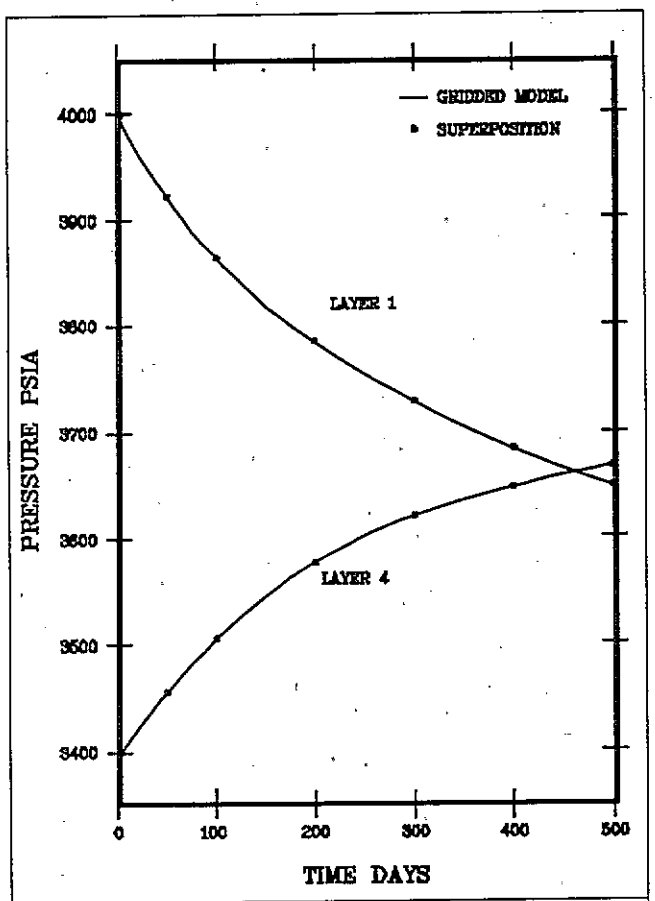

Fig. 7—Pressure-transient comparison of gridded model and superposition method.

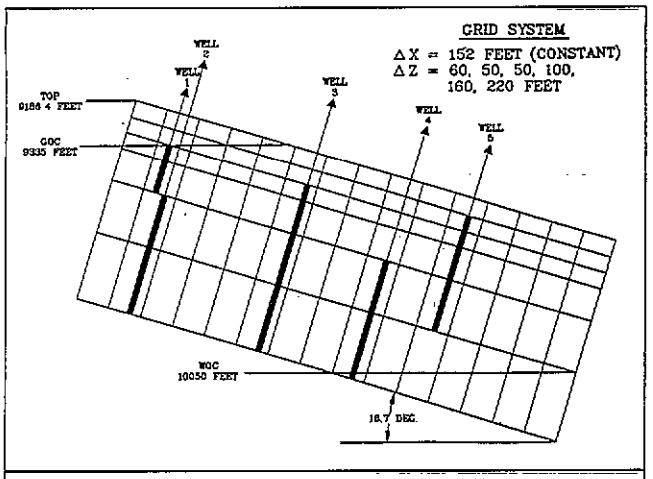

Fig. 8—Grid system details for field example.

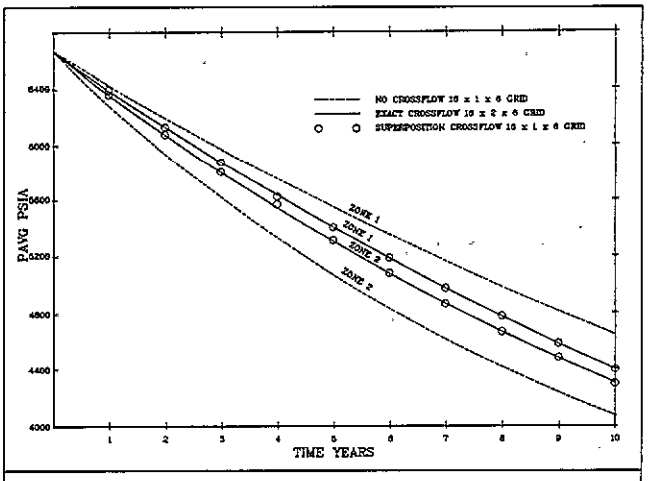

Fig. 9—Pressure vs. time for field-scale cross section.

requires input data specifying water, oil, and gas k_r and viscosity values; PI; and pressure for each layer. Well rate, q, and withdrawal point (layer) also require specification.

This stand-alone program allowed many cases with different sets of input data to be run rapidly. In all cases, the superposition method gave somewhat better to much better agreement with exact results than the mixed-wellbore method. Only one three-phase example is presented here. **Table 1** gives fluid and reservoir layer data for a well completed in eight reservoir grid layers. Layer pressures are far from equilibrium, varying from 1,500 to 6,000 psia. Pressures and phase mobilities were assigned arbitrarily throughout the layers. Note that the only communication between layers is through the wellbore.

Results are presented for well rates of 1,000 and 0 RB/D, with withdrawal from the wellbore in the top layer. **Fig. 1** shows the layer total flow rates for the case of $q=1{,}000$ RB/D. Positive rates represent production (inflow) into the wellbore, and negative rates represent outflow into the formation. All three methods give the same layer (total) rates and flowing wellbore pressure, $p_w=3{,}608$ psia, and the arithmetic sum of the layer rates is 1,000.

Figs. 2 and 3 compare the outflow-layer individual gas- and water-phase rates. Inflow-(producing)-layer phase rates are omitted because all three methods give identical values of those rates, as previously mentioned. Figs. 2 and 3 show better agreement with exact results for the superposition method than for the mixed-wellbore method. The overall crossflow rate, defined as total inflow rate minus well rate, for this case is 1,909 RB/D for all three methods.

Figs. 4 through 6 show results for the shut-in case where crossflow is a maximum. Fig. 4 shows the layer total flow rate profile

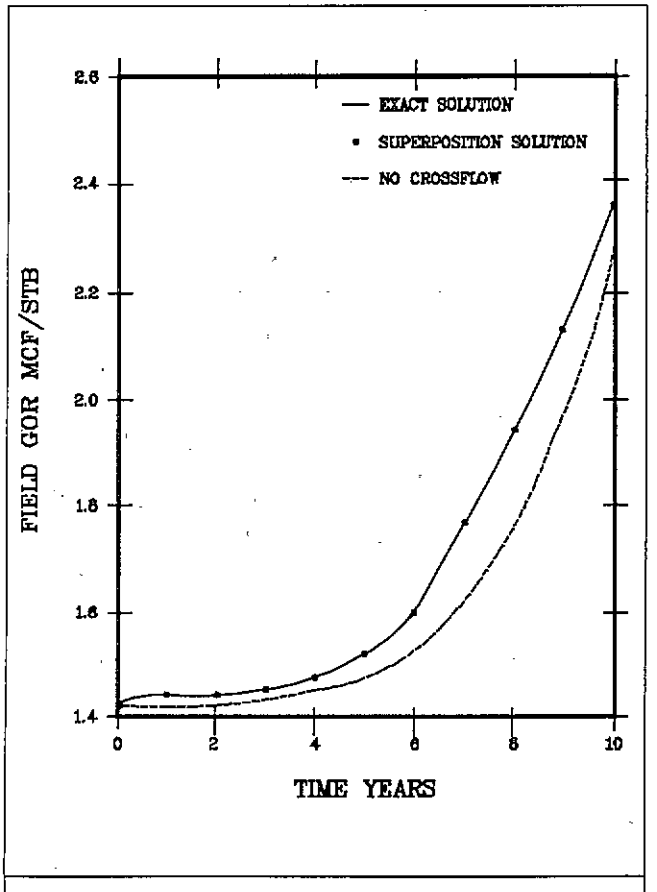

Fig. 10—Field GOR.

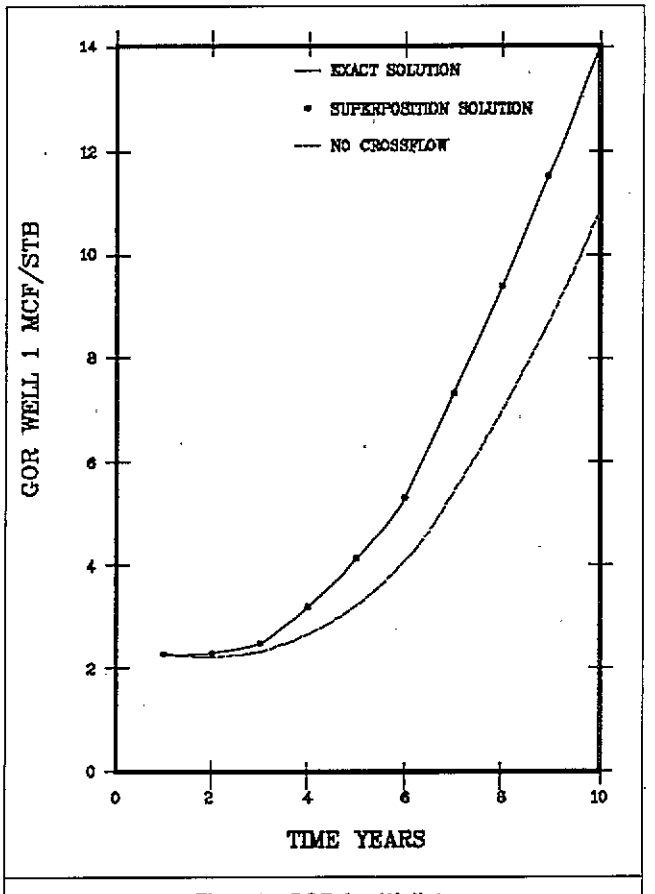

Fig. 11—GOR for Well 1.

TABLE 5—COMPOSITIONAL DATA FOR FIELD EXAMPLE PROBLEM*

Number of components = 6 (C_1, C_2, C_3, C_4, C_{5-6}, C_{7+})

Bubblepoint Variation With Depth

Elevation (ft ss)	Bubblepoint (psia)	Initial Compositions					
9,335	6,568.4	0.65987	0.09298	0.04309	0.02189	0.03369	0.14217
9,400	6,500.0	0.65481	0.09305	0.04329	0.02846	0.03413	0.14626
9,600	5,650.0	0.59522	0.09349	0.04561	0.03163	0.03946	0.19460
9,800	4,600.0	0.52027	0.09277	0.04829	0.03570	0.04678	0.25620
10,100	2,450.0	0.33037	0.08210	0.05261	0.04595	0.06899	0.41999
11,000	2,000.0	0.28030	0.07626	0.05231	0.04807	0.07538	0.46768

Properties at Reservoir Conditions and 6,568.4 psia

Oil molecular weight, lbm/lbm mol	50.69
Gas molecular weight, lbm/lbm mol	27.75
Oil density, lbm/ft^3	32.42
Gas density, lbm/ft^3	21.10
Oil z factor	1.3585
Gas z factor	1.1420
Oil viscosity, cp	0.0948
Gas viscosity, cp	0.0434

*The full set of PVT data is not included in the paper owing to space limitations. These data are available from the authors upon request.

TABLE 6—SATURATION DATA FOR FIELD EXAMPLE

Water Saturation	k_{rw}	k_{row}	P_{cwo}
0.11	0.000	1.000	1.000
0.30	0.005	0.400	0.200
0.40	0.020	0.180	0.100
0.50	0.050	0.080	0.050
0.60	0.100	0.020	0.010
0.70	0.250	0.007	0.005
0.76	0.350	0.000	0.000
1.00	1.000	0.000	0.000

Liquid Saturation	k_{rog}	k_{rg}	P_{cgo}
0.11	0.0000	1.0000	4.000
0.26	0.0000	0.4000	2.500
0.35	0.0002	0.3600	1.500
0.41	0.0017	0.3300	1.050
0.51	0.0130	0.2100	0.796
0.54	0.0210	0.1600	0.720
0.61	0.0500	0.1110	0.650
0.64	0.0760	0.0900	0.620
0.71	0.1367	0.0550	0.585
0.74	0.1873	0.0400	0.570
0.81	0.3052	0.0327	0.513
0.85	0.4212	0.0200	0.480
0.91	0.5953	0.0133	0.460
0.94	0.7300	0.0100	0.450
1.00	1.0000	0.0000	0.430

and Figs. 5 and 6 show the outflow gas- and water-phase rate profiles. These figures show better superposition/exact method agreement than for the previous case with $q=1{,}000$ RB/D. Also, the relative accuracy of the superposition vs. the mixed-wellbore method is greater than in the previous case. The overall crossflow rate is 2,395 RB/D.

Table 2 shows the calculated wellbore saturation profiles for the 1,000- and 0-RB/D well rate cases obtained from the exact solution. The superposition method wellbore saturations equal the exact saturations for the shut-in case and are close to the exact values for the flowing case. The mixed-wellbore method gives a single set of saturations for the entire wellbore.

In this particular example, the oil outflow rates were much smaller than the gas and water rates and are omitted for brevity. The accuracy of the outflow-layer oil rates is similar to that of the gas and water rates.

Transient Response to Shut-In With Crossflow. A second procedure for examining the accuracy of the superposition method is use of the simulator to compare field-scale transient behavior calculated "exactly" and that calculated with the superposition method. Simulator results "exactly" reflecting crossflow are obtained in the following manner for 2D r-z single-well or 2D x-z cross-sectional cases. The wellbores are included directly in the grid. Vertical permeability in each wellbore is very large to achieve negligible or small vertical viscous pressure gradients in the wellbore. Wellbore cell volumes are very small, reflecting actual wellbore radius. The transmissibility connecting a wellbore cell to its adjacent matrix gridblock equals the layer PI of that wellbore layer. No-slip flow (fractional flow=saturation) is used vertically within each wellbore and for lateral flow out of a wellbore cell into its adjacent matrix gridblock. Zero capillary pressure is used in wellbore cells. While each wellbore cell is a distinct cell in the grid, it represents a wellbore in the center of its adjacent matrix gridblock. This approach accounts rigorously for wellbore pressure gradient and includes compressibility and mass-transfer effects within the wellbore. Further explanation is given in the two examples below.

The simulator used here is a previously described fully implicit compositional model.[4] Detailed equation-of-state PVT data for the examples below are omitted for brevity but are available from the authors.

TABLE 7—FIELD EXAMPLE WELL DATA

Well	Oil Rate (STB/D)	Individual Layer J_k				
		2	3	4	5	6
1	200	—	0.6962	1.490	—	—
2	600	—	—	—	0.8355	0.4787
3	800	—	0.6962	1.490	0.8355	0.4787
4	1,000	—	—	—	0.8355	0.4787
5	150	0.5439	0.6962	1.490	0.8355	—

Our second example used the simulator to calculate a simple single-phase well transient. A well is completed in four layers at the center of a cylinder with r_w=0.25 ft and closed r_e=564.2 ft. Vertical permeability is zero, so the layers communicate only through the wellbore. For each layer, the thickness and the PI are 200 ft and 0.2032 RB-cp/D-psi, respectively. Porosity is 0.2, S_w=0.2 (immobile), S_o=0.8, and k_{ro}=1.0. Initial pressures in Layers 1 through 4 are 4,000, 3,800, 3,600, and 3,400 psia, respectively. Corresponding initial oil viscosities are 0.1549, 0.1477, 0.1399, and 0.1326 cp. Oil gradient at the initial average pressure of 3,700 psia is 0.2322 psi/ft.

The first model run was on a 1×4 r-z (1D vertical) grid with the superposition method activated to allow crossflow. The second model run used a 2×4 r-z grid. The first radial increment represented the wellbore; the second radial increment represented the reservoir (matrix). This second 2×4 run represents the exact solution in this example. Each layer's radial transmissibility was 0.2032 RB-cp/D-psi.

Fig. 7 shows calculated pressures for Layers 1 and 4 vs. time for the two model runs. The superposition method pressures are virtually identical to the 2×4 grid model results. The other two layers show equally good agreement.

Ten-Year Depletion of Field-Scale Cross Section. The third test example for the superposition method is a field-scale x-z cross section 2,432 ft in length and 2,800 ft wide with a total thickness of 640 ft. The cross section has a constant dip angle of 16.7°. **Fig. 8** shows the 16×6 x-z grid. **Table 3** gives reservoir stratification and properties. A shale barrier between Layers 4 and 5 separates the structure into two isolated zones that communicate only through wellbores. This fact, together with low vertical permeability throughout, gives rise to significant crossflow effects.

Table 4 gives additional reservoir data, including initial pressure and water/oil contact (WOC) and gas/oil contact (GOC) depths. The initial bubblepoint varies with depth from 6,558 psia at the GOC to 2,000 psia at the bottom of the structure, as shown in **Table 5. Table 6** gives relative permeability and capillary pressure data. Fig. 8 shows the five producing wells, and **Table 7** gives additional well information. Since vertical permeability is zero between Layers 4 and 5, we define Zone 1 as the top four layers and Zone 2 as the bottom two layers. Well 1 is completed only in Zone 1, Wells 2 and 4 only in Zone 2, and Wells 3 and 5 are perforated in both zones. The only interzone communication is therefore through the wellbores of Wells 3 and 5.

The exact model run used a 3D 16×2×6 grid with the second (y-direction) slice simulating the wellbores. The second slice contains only wellbores with all PV's zero except all cells adjacent to the original well locations. Wells are completed only in the second slice. Vertical wellbore permeabilities are very large to minimize vertical wellbore viscous gradients, and y-direction transmissibilities are equal to the well PI's at the wellbore cell locations. Wellbore cell volumes reflect actual wellbore radii. In summary, the second slice was added to model the wellbores in the reservoir rigorously.

Three 10-year simulation runs were made with the well rates given in Table 7. One run was made with the exact 3D 16×2×6 grid. A second run was made with the superposition method activated for all wells, and a third run was made allowing no crossflow. These last two runs used the 2D 16×6 x-z grid. In the third run, when a layer tried to accept fluid from a wellbore, the layer simply was shut in.

Fig. 9 shows the average pressure vs. time for both zones and all three simulation runs. The values from the exact solution and the superposition method are virtually identical, while the shut-in-procedure results vary significantly from the true solution. After 10 years, the correct solution gives a 98-psia difference in pressure between the two zones, while merely shutting in crossflowing layers gives a pressure difference of 582 psia. **Fig. 10** shows the field average GOR vs. time for the three runs, where again the excellent agreement between the exact and superposition methods may be seen. **Fig. 11** shows a similar plot for the highest GOR well (Well 1). Again, excellent agreement may be observed. No results are shown for water production because this particular problem produced little water.

Because the mixed-wellbore method is unavailable in the simulator, it is difficult to comment or to predict what this method would have done in this simulation. However, the results presented earlier on the instantaneous individual phase rates showed significant differences between the methods.

Conclusions

1. Reservoirs exhibiting significant wellbore crossflow require simulators that accurately treat crossflow to predict correct reservoir performance. Simply shutting in backflowing layers may yield erroneous results.
2. The superposition method appears to be a good compromise between a shut-in procedure and a full simulation of the wellbore within the grid. The method is reasonably accurate and relatively straightforward to implement in a reservoir simulator.
3. The superposition method does not require additional matrix algebra and therefore costs little in computing time or storage.

Nomenclature

J_k = well layer PI, RB-cp/D-psi
k_r = relative permeability, fraction
p_k = reservoir pressure at Layer k, psia
p_w = wellbore pressure, psia
p_w^* = layer shut-in method wellbore pressure, psia
p_{wk} = wellbore pressure at Layer k, psia
Δp_{wk} = wellbore gradient term, psi
P_c = capillary pressure, psi
P_k = $pk-\Delta p_{wk}$, psi
$\hat{P}_k$ = minimum of P_k and p_w^*, psia
q = total target well production rate, RB/D
q_k = total flow rate at Layer k, RB/D
$\hat{q}_k$ = layer flow rates that sum to zero over layers, RB/D
q_k^* = layer shut-in method rate at Layer k, RB/D
q_{kj} = flow rate between Layers k and j, RB/D
q_{mk} = flow rate of Phase m at Layer k, RB/D
r,z = radial coordinates
r_e = exterior radius, ft
r_w = wellbore radius, ft
S = saturation, fraction
S_m^{wb} = average wellbore saturation of Phase m, fraction
S_{mk}^{wb} = wellbore saturation of Phase m at Layer k, fraction
T_{kj} = transmissibility between Layers k and j, RB-cp/D-psi
x,y = coordinates
λ_k = total three-phase mobility at Layer k, cp^{-1}
$\hat{\lambda}_k$ = upstream total mobility at Layer k, cp^{-1}
$\hat{\lambda}_{mk}$ = upstream mobility for Phase m at Layer k, cp^{-1}
μ = viscosity, cp
ϕ_k = flow potential at Layer k, psi

Subscripts

k,j = Layer k or j
m = water, oil, or gas phase
w = wellbore value
w,o,g = water, oil, gas

Superscripts

ma = value within reservoir or matrix
wb = value within wellbore

Acknowledgments

We are grateful to C.A. Ellis, D.C. Leo, and M.A. Martinez for aid in preparing the paper and figures. We also thank Scientific Software-Intercomp for permission to publish the paper.

Authors


Modine


Coats


Wells

Alan D. Modine, deceased, was a vice president of Scientific Software-Intercomp in Houston, TX, currently involved in the development and applications of reservoir simulators. He had 30 years' experience in reservoir engineering and simulation. Modine holds a BS degree from the U. of Illinois and MS and PhD degrees from Carnegie-Mellon U., all in chemical engineering. **K.H. Coats** worked in simulation R&D for Scientific Software-Intercomp. He holds BS, MS, and PhD degrees in chemical engineering and an MS degree in mathematics from the U. of Michigan. A Distinguished Member, Coats received the 1984 Lester C. Uren Award and the 1988 Anthony F. Lucas Gold Medal. He was a 1969–70 Distinguished Lecturer and a member of the 1977–78 Nominating and 1984–86 Reprint Series committees. **Mike Wells**, now with Intera ECL-Petroleum Technologies in Denver, was development manager in the Reservoir Simulation Group at Scientific Software-Intercomp. His main areas of responsibility were production algorithms, extended black-oil models and simulation pre- and postprocessing. He previously worked in the Energy Div. of Scicon. He holds a BS in mathematics from the U. of Bristol, UK.

References

1. Trimble, R.H. and McDonald, A.E.: "A Strongly Coupled Fully Implicit Three-Dimensional Three-Phase Well Coning Model," *SPEJ* (Aug. 1981) 454–58.
2. Bansal, P.P. *et al.*: "A Strongly Coupled, Fully Implicit, Three-Dimensional, Three-Phase Reservoir Simulator," paper *SPE 8329* presented at the 1979 SPE Annual Technical Conference and Exhibition, Las Vegas, Sept. 23–26.
3. Holmes, J.A.: "Enhancements to the Strongly Coupled, Fully Implicit Well Model: Wellbore Crossflow Modeling and Collective Well Control," paper SPE 12259 presented at the 1983 SPE Symposium on Reservoir Simulation, San Francisco, Nov. 15–18.
4. Coats, K.H.: "Implicit Compositional Simulation of Single-Porosity and Dual-Porosity Reservoirs," paper SPE 18427 presented at the 1989 SPE Symposium on Reservoir Simulation, Houston, Feb. 6–8.

SI Metric Conversion Factors

bbl	× 1.589 873	E−01	=	m^3
cp	× 1.0*	E−03	=	Pa·s
ft	× 3.048*	E−01	=	m
ft^3	× 2.831 685	E−02	=	m^3
°F	(°F−32)/1.8		=	°C
lbm	× 4.535 924	E−01	=	kg
md	× 9.869 233	E−04	=	μm^2
psi	× 6.894 757	E+00	=	kPa
psi^{-1}	× 1.450 377	E−01	=	kPa^{-1}

*Conversion factor is exact.

SPERE

Original SPE manuscript received for review Sept. 2, 1990. Revised manuscript received July 19, 1991. Paper accepted for publication Aug. 5, 1991. Paper (SPE 20746) first presented at the 1990 SPE Annual Technical Conference and Exhibition held in New Orleans, Sept. 23–26.

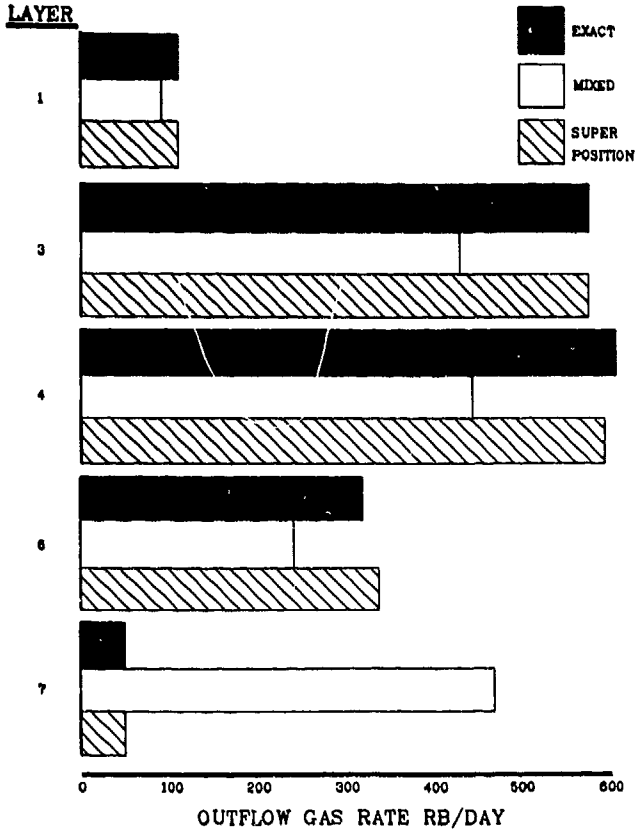

FIG. 5 - RESULTS FOR SHUT-IN WELL

FIG. 6 - RESULTS FOR SHUT-IN WELL

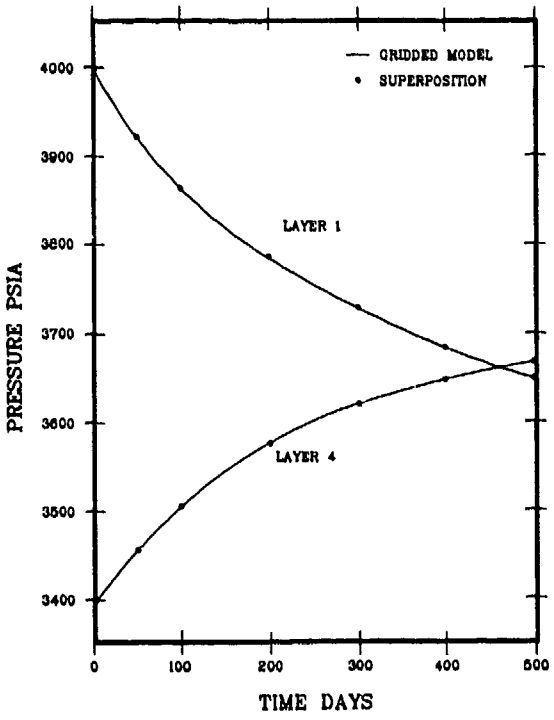

FIG. 7 - PRESSURE TRANSIENT COMPARISON OF GRIDDED MODEL AND SUPERPOSITION METHOD

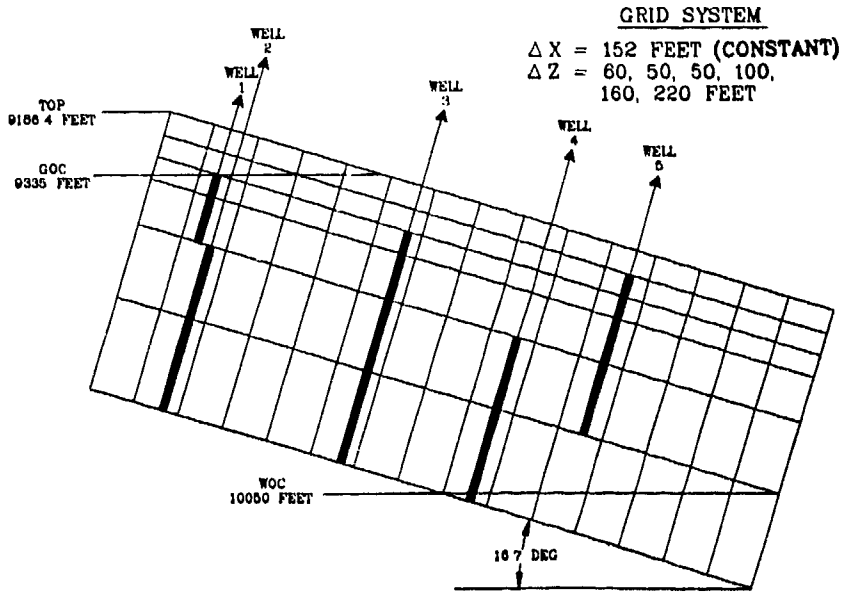

FIG. 8 - GRID SYSTEM DETAILS FOR FIELD EXAMPLE

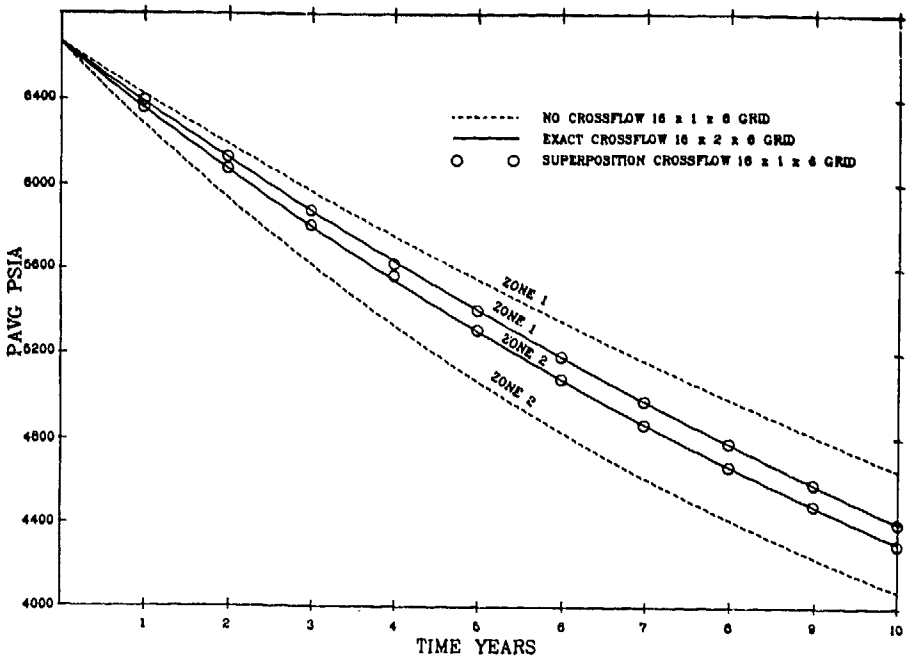

FIG. 9 - PRESSURE VS TIME FOR FIELD-SCALE CROSS-SECTION

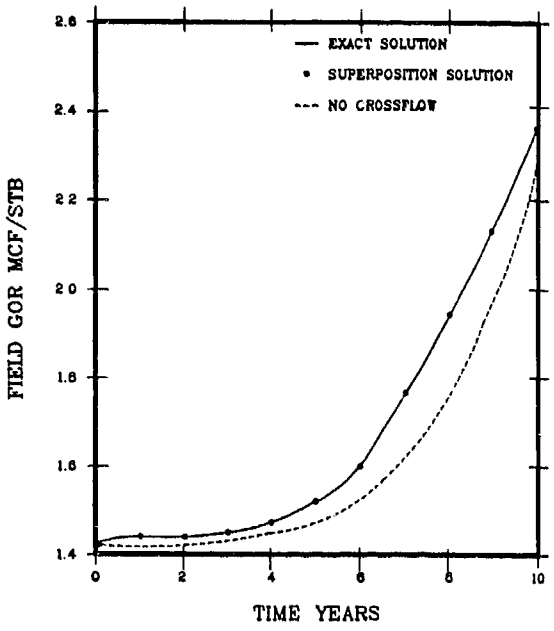

FIG. 10 - FIELD GAS-OIL RATIO

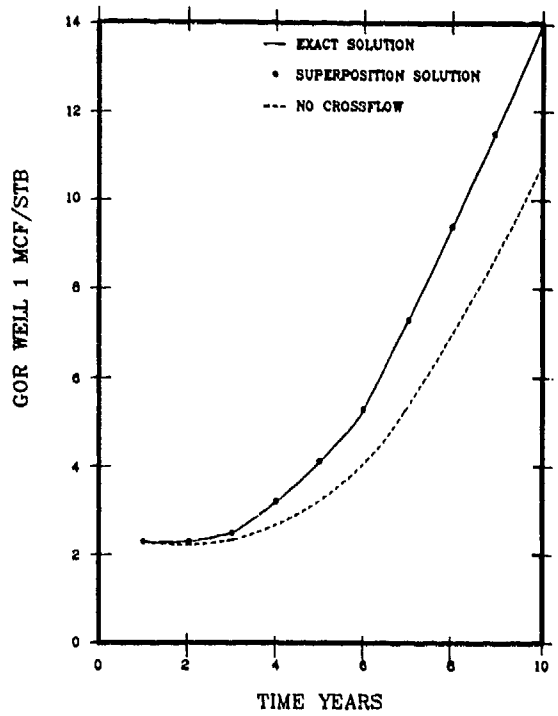

FIG. 11 - GOR FOR WELL 1